RSC Advances

ROYAL SOCIETY OF CHEMISTRY

www.rsc.org/advances

Journal Name

ARTICLE

Nanoassembly of an Amphiphilic Cyclodextrin and Zn(II)-Phthalocyanine with the Potential for Photodynamic Therapy of Cancer

Claudia. Conte, [a] Angela Scala, [b] Gabriel Siracusano,[c] Nancy Leone,[d] Salvatore Patanè,[e] Francesca Ungaro,[a] Agnese Miro,[a] Maria Teresa Sciortino,[c] Fabiana Quaglia,[a]* and Antonino Mazzaglia[b]*

Due to their poor solubility and propensity to aggregate in aqueous media, therapeutic application of several photosensing agents, such as phthalocyanines, in photodynamic therapy (PDT) of solid tumors is severely hampered. With the aim to propose a novel nanotechnological approach, in this paper biodegradable nanoassemblies based on heptakis (2-oligo(ethyleneoxide)-6-hexadecylthio-)-β-CD (SC16OH) and zinc-phthalocyanine (ZnPc) were developed and tested. Nanoassemblies, prepared by the emulsion-solvent evaporation technique, displayed a hydrodynamic diameter around 200 nm, a negative zeta potential and a satisfactory entrapment efficiency of ZnPc. Steady-state and time resolved fluorescence emission spectroscopy studies showed the entrapment of ZnPc as a monomer in the carrier, with a low tendency to self-aggregate and consequently a fairly good propensity to generate singlet oxygen after photoactivation. The interaction of ZnPc with SC16OH was elucidated by ^{1}H-NMR, which suggested the formation of complexes between drug and both hydrophobic and hydrophilic moieties of the amphiphle. Finally, in vitro potential of the nanoassembly was evaluated in HeLa cells by following cellular uptake and photobiological activity. Overall, results suggest the suitability of nanoassembly based on SC16OH for delivering ZnPc to cancer cells, thus inducing photodynamic anticancer effects.

Introduction

Conventional anticancer therapy is associated to multiple drawbacks and severe side effects which have required intensive efforts aimed at optimizing the therapeutic outcome. Alternative therapeutic options such as photodynamic therapy (PDT) are opening a new avenue in the localized treatment of solid tumors via light exposure.[1] PDT relies on the administration of a photosensitizer (PS) which can be activated by light of a specific wavelength, resulting in a sequence of photochemical processes, finally generating cytotoxic species. Amid them, singlet oxygen elicits remarkable destruction of cell structures and irreversible photodamage of tumor tissue though different molecular mechanisms.[2] Despite the obvious promise shown by PDT in cancer therapy and in analogy to most anticancer drugs, PS are often characterized by a disadvantageous physico-chemical profile which narrows their clinical application.[3] Their high lipophilicity and propensity to fast aggregation in aqueous media strongly depress their

photobiological activity. Furthermore, one of the main challenges in PDT is to maximize drug dose at diseased site while attenuating toxicity profile.

Phthalocyanines are currently being intensively investigated as potential photosensitizers for PDT. Since they strongly absorb light in the red and near infrared (NIR) regions of the visible spectrum which correspond to the tissue optical window, they can in theory be activated within deeper tissue regions. In addition, their minimal absorption at 400–600 nm would minimize the effects of skin photosensitization caused by sunlight. However, their use in clinical PDT is limited by their poor water solubility and strong tendency to form aggregates.[4,5]

The use of cyclodextrins (CDs) in this field has attracted increasing interest, prompted by their ability to act as hosts for several hydrophobic molecules. Being characterized by an internal hydrophobic cavity, CDs can accommodate well-fitting groups through the combination of hydrophobic, van der Waals and hydrogen-bonding interactions, thus forming non-covalent inclusion complexes with distinctive biological properties.[6]

Recently, research efforts have been devoted to the design and synthesis of macrocyclic amphiphiles of hydrophobically modified CDs obtained by functionalizing primary and/or secondary rim with linear or branched aliphatic chains of different lengths (C2–C18) through different chemical bonds (ester, ether or amide).[7] CD amphiphilic derivates (aCD), which can be non-ionic, cationic or anionic, are prone to give a wide array of supramolecular nanostructures through self-assembly or by incorporation in lipid membranes, including monolayers, vesicles, micelles with great potential as drug delivery nanoconstructs.[3-6,8-11] Organization of self-assembled aCDs is driven by the balance between hydrophobic and hydrophilic moieties and depends on the nature and length of the grafted chains at the different sides. For example, the introduction of lipophilic alkylthio "tails" and oligo(ethylene glycol) "head groups" leads to the formation of non-ionic vesicles in water, which were characterized by a strong colloidal stability as well as a potentially low immunogenic effect.[10,12]

Various natural or synthetic CDs, including amphiphilic CDs, have been extensively studied in in the delivery of phtalocyanines,[13-15] porphyrins,[16,17] and curcumin.[18,19] to overcome their main therapeutic restrictions, including chemical conjugation or entrapment in colloidal nanocontainers.[20,21] Ravoo's group reported a self-assembly based on an adamantane-functionalized, hexaanionic water-soluble zinc(II) phthalocyanine (PC) inserting on the surface CD vesicles.[22] Furthermore, several non-ionic and cationic amphiphilic derivates of β-CD assemblying in supramolecular nanostructures able to host ~~both hydrophobic and~~ hydrophilic PS have been recently investigated.[23-26]

Generally, this class of aCD shows high versatility towards PS complexation [26] as well the potential to target biological sites.[27] or to be modified with stimuli-responsive groups.[28] These premises prompt toward the use of engineered multifunctional nanoconstructs based on aCD in therapy, diagnosis, and biosensing.

With the aim to design novel photherapeutic nanoassemblies, our recent results mainly rely with model systems based on the self-assembly in aqueous solution of aCDs and negatively charged porphryins. To the best of our knowledge, the design of a photosensitizing nanosystem based on aCD and a water insoluble PS, widely utilized for PDT, has not been reported yet.

Along this direction here we propose a CD nanoassembly embedding the highly hydrophobic PS ZnPc (Scheme 1).
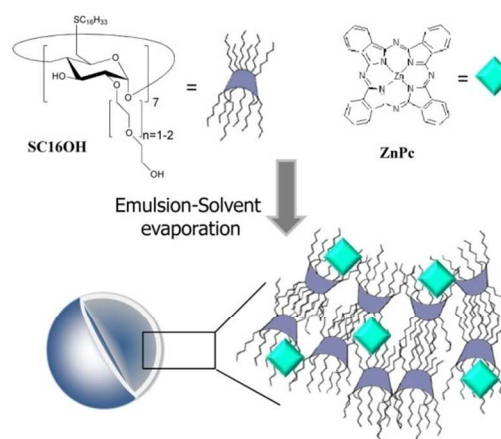
Scheme 1: Molecular structure of SC16OH, ZnPc and corresponding ZnPc/SC16OH nanoassembly.

The system was prepared by emulsion–solvent evaporation method and characterized in term of size, surface charge, morphology and release properties. Emitting features of the nanoassembly were evaluated by pointing out at the entrapment of ZnPc as a monomer and its propensity to appreciably generate singlet oxygen. NMR studies gave insight on complex between amphiphile and ZnPc elucidating the assistance of both hydrophobic and hydrophilic moiety of amphiphilic CD in the formation of the nanoassembly. Finally, in vitro uptake and photoactivation of the nanoassembly were evaluated in HeLa cells.

Experimental

Materials

Heptakis (2-oligo(ethyleneoxide)-6-hexadecylthio-)-β-CD (SC16OH, MW(10EO)=3435.30 da, EO= ethylenoxide units) was synthesized as reported elsewhere.[29] Zinc(II) phthalocyanine (ZnPc, MW= 577.91), Nile Red (NR, MW= 318.38), Polysorbate 80, anthracene-9,10-dipropionic acid (ADPA), potassium phosphate dibasic and potassium phosphate monobasic, sodium azide and sodium chloride were purchased from Sigma-Aldrich. Sodium hydroxide was provided from Delchimica Scientific Glassware. Ethanol 96°, phosphoric acid (85%), acetonitrile and tetrahydrofuran were purchased from Carlo Erba Reagenti (Milan, Italy). RPMI enriched with FBS 10% was used as cell culture medium.

Preparation of ZnPc/SC16OH

Nanoassembly was prepared by an emulsion–solvent evaporation method. SC16OH (10 mg) and ZnPc (20 μg corresponding to 0.2% of SC16OH weight) were dissolved in DCM:THF 9:1 (1 mL). This solution was poured in water (10 mL) and sonicated for 2 min at 3W (Sonicator 3000, Misonix, USA) by a microtip probe under controlled temperature of 4 °C. Thereafter, the organic solvent was evaporated by mechanical stirring for 4 h at room temperature. Nanoassembly

was collected by ultracentrifugation (278000 x g, 30 min, 4 °C) after washing twice with distilled water to remove unencapsulated drug. Nanoassembly was then redispersed in water (2 mL), freeze-dried for 24 h (Modulyo, Edwards,UK) and kept at 4°C. Recovery yield of production process was evaluated by weighting the solid residue after freeze-drying. Results are expressed as the ratio of the actual nanoassembly weight to the theoretical SC16OH weight x 100.

~~ZnPc loading was evaluated by dissolving a known amount of freeze-dried nanoassembly (1 mg) in 1 mL of THF under magnetic stirring for 1 h and analysing the solution as previously described.[30]~~

Characterization of ZnPc/SC16OH

Hydrodynamic diameter (DH) and polydispersity index (PI) of nanoassembly were determined by Photon Correlation Spectroscopy (PCS) using a N5 Submicron Particle Size Analyzer (Beckman-Coulter). A nanoassembly dispersion was diluted in Milli-Q water at intensity in the range 104-106 counts/s and measurements were performed at 25°C on 90° angle. Results are reported as mean DH of three separate measurements of three different batches (n=9) ± SD.

Zeta potential was determined by analysing a nanoassembly dispersion in water on a Zetasizer Nano Z (Malvern Instruments Ltd.). Results are reported as mean of three separate measurements of three different batches (n=9) ± SD.

The morphology of NPs was examined by transmission electron microscopy (CM 12 Philips, The Netherlands) using samples stained with a 2% phosphotungstic acid solution.

Scanning Near-Field Optical Luminescence (SNOL) measurements were performed using a homemade setup based on a Zeiss optical microscope. A laser beam at 532 nm was coupled to a bended optical fiber that locally illuminates the sample in the near field regime. The distance between the sample and the nano-aperture of the optical fiber was kept constant by a feedback based on a tuning fork mechanism. The laser light was filtered out placing a razofilter at 533 nm in the optical path and the luminescence was detected by a phototube connected to the video port of the microscope. Sample was prepared by diluting (about 1:4) in ultrapure water nanoassembly dispersion up to 0.5 mg/mL. After 1 h of sonication, a drop of dispersion was casted on Si (100) surface. SNOL images were reported by using green colour which is conventionally used to increase the contrast between differently luminescent regions.

ZnPc loading was evaluated by dissolving a known amount of freeze-dried nanoassembly (1 mg) in 1 mL of THF under magnetic stirring for 1 h and analysing the solution as previously described.[28]

Fluorescence studies

Fluorescence spectra of ZnPc/SC16OH dispersed in ultrapure water (Galenica Senese, V=10 mL) were collected. Fluorescence spectra on free ZnPc in DMSO and ZnPc/SC16OH dispersed in CHCl$_3$ and in DMSO, respectively were registered too. In all the experiments, ZnPc concentration

was set at 0.25 µg/mL. Steady-state fluorescence measurements were performed on a Jasco model FP-750 spectrofluorimeter. Emission spectra were carried out by using an excitation wavelength of 600 nm. Excitation spectra were carried out on emission band at 700 nm. A 1 cm path length quartz was used. Fluorescence spectra were corrected for the amount of adsorbed light at the excitation wavelength and for scattering of the samples, this latter by subtracting a correspondent scattering function (Origin 8.0).

Time-resolved fluorescence measurements were carried out by a time-correlated-single-photon-counting (TCSPC) home-made apparatus.[31,32] The collected data were then analyzed using the non-linear least-squares iterative reconvolution procedures based on the Marquardt algorithm. In the case of total fluorescence decay curves, the fitting was performed on the basis of the multiexponential decay law[32]

$$I(t) = I_0 \sum_i \alpha_i \exp(-t/\tau_i) \tag{1}$$

where I(t) is the total fluorescence decay curve, I$_0$ is the intensity at time zero, and α_i and τ_i are, respectively, the relative amplitudes and lifetimes of the ith component (the normalization condition is). Static and time- resolved fluorescence anisotropy r(t) was measured as previously reported[32] (see ESI material).

NMR studies

NMR spectra were recorded on a Varian 500 MHz spectrometer at room temperature (r.t $\cong$ 25°C). The chemical shifts (δ) are expressed in ppm. Samples were prepared as follow: 1 mg of ZnPc was dissolved in 1 mL of d$_6$-DMSO; 8 mg of ZnPc/SC16OH were dispersed in 1 mL of CDCl$_3$ leading to ZnPc/SC16OH complex.

ZnPc: ^{1}H-NMR (500 MHz, d$_6$-DMSO): δ = 8.27 (s, 8H), 9.44 (s, 8H).

SC16OH: ^{1}H-NMR (500 MHz, CDCl$_3$) δ = 0.88 (t, 21H, CH$_3$), 1.30 (br s,182 H, CH$_2$), 1.57 (m, 14H, CH$_2$), 2.00 (br, OH), 2.60 (m, 14H, SCH$_2$), 3.00 (m, 14H, H6), 3.3-4.0 (m, ca. 84H, H2-5 and OCH$_2$CH$_2$O), 5.05 (br, 7H, H1).

ZnPc/SC16OH: ^{1}H-NMR (500 MHz, CDCl$_3$) shifted peaks: δ = 8.10 (s, Ar-H), 8.20 (s, Ar-H), 9.50 (s, Ar-H), 9.78 (s, Ar-H).

Singlet oxygen generation from ZnPc/SC16OH

The capacity of nanoassembly to generate singlet oxygen was monitored over time by measuring photobleaching of the radical quencher ADPA.[33]Briefly, 40 µL of a 5 mM ADPA solution in 0.01 M NaOH were added to 2 mL of a ZnPc (2 µg/mL in THF/H$_2$O 1:100) or a nanoassembly aqueous dispersion (1 mg/mL). The sample was irradiated at 610 nm using a 150 W ozone-free xenon-arc lamp (Jobin Yvon) with a slit width of 10 nm for different times (15, 30 and 45 min). All the solutions are optically matched at the excitation wavelength (610 nm). Sample containing nanoassembly was centrifuged at 16090 x g (Mikro 20, Hettich) for 30 minutes. The supernatant was collected and analysed by spectrophotometry at 400 nm to

evaluate ADPA absorption. The production of singlet oxygen was monitored by the decrease of OD at 400 nm as a function of the irradiation time. Results are reported as ratio between sample OD after irradiation and sample OD before irradiation. The mean of three independent experiments ± SD is reported.

Cell culture

HeLa cells were obtained from the American Type Culture Collection and propagated at 1:6 ratio in RPMI-1640 supplemented with 100 units/mL of penicillin and 10% fetal bovine serum (FBS).

Uptake of nanoassembly

Approximately 1×10^5 HeLa cells were grown in 6 wells plates. After overnight incubation, cells were incubated for 1 h at 4° C and 37°C separately with Nile Red-nanoassembly (10 μg/mL). Cells were washed by PBS, detached and placed into a slide treated with polylysine. Cells were finally analysed by fluorescence microscopy.

Photodynamic activity

Cells were grown in 6 well-plates and after 24 h treated with ZnPc dissolved in DMSO (0.012 μg/mL), ZnPc/SC16OH and unloaded nanoassembly (10 μg/mL) at 37°C. Cells were subsequently detached from the substrate using trypsin, transferred in polystyrene tubes and centrifuged. After washing in PBS, cell pellets were re-suspended in PBS and placed separately in a spectrophotometric cuvette to be irradiated with a halogen lamp for 30 min. The irradiating beam was filtered through an UV filter (Hoya glass type UV-34, cut-off: 340 nm) in order to cut the UV component and through a 1 cm cell filled with water, to remove the IR-component. A light dose of $\cong 5$ joule/cm^2 was estimated. After 24 h of incubation, treated cells were placed in 96-well plates with 100 μL RPMI-1640 medium in the presence of a tetrazolium compound [3-(4,5-dimethylthiazol-2-yl)-5-(3-carboxymethoxyphenyl)-2(4-sulfophenyl)-2H tetrazolium, inner salt; MTS, Promega] and an electron coupling reagent phenazinemethosulfate (PMS) dye (MTS at 20 μL per well). As control, cells were exposed to the vehicle alone (DMSO) in amounts corresponding to those employed for dissolving the compounds. After further incubation (1 h), the absorbance was read at 490 nm in a microplate reader (Lab system Multiskan Bichromatic). The percentage of cell viability (%) was calculated according to the equation:

Cell viability (%) = [(OD before lamp-OD after lamp)/OD before lamp]x100

Results and discussion

Preparation and characterization of ZnPc/SC16OH nanoassembly

On the basis of our previous findings on SC16OH propensity to form vesicular nanoassemblies able to deliver lipophilic drugs,[34] in this study we prepared a nanoassembly containing ZnPc (ZnPc/SC16OH, Scheme 1) by the emulsion-solvent evaporation technique. During the preparation process, all the materials were co-dissolved in an organic phase composed by DCM and a small amount of THF, in order to promote the solubilization of the strongly lipophilic cyanine. Initial ZnPc/SC16OH weight ratio was fixed at 1:500 since higher ZnPc amounts could not be solubilized in the THF/DCM solution. Recovery yield of preparation process, size, polydispersity index, zeta potential and ZnPc loading of nanoassembly are summarized in Table 1. As clearly shown, properties of the nanoassembly were not significantly affected by the presence of PS. Recovery yield of the formulations was around 80%, evidencing that during the preparation of nanoassembly, PS and SC16OH macroscopic aggregation did not occur.

Table 1. Overall properties of SC16OH nanoassemblies. SD was calculated on three different batches.

	Unloaded-SC16OH nanoassembly	ZnPc/SC16OH nanoassembly
ZnPc (% w/w)	-	0.2
Yield (%)	84	77
Mean D_H (nm ± SD)	215±10	200±10
P.I.	0.144	0.221
Zeta Potential (mV ± SD)	-26.6±3.5	-25.6±2.5
ZnPc Actual loading[a] (Ent. Efficiency[b])	-	0.152 ± 0.04 (76.0± 13.8)

[a]Actual loading is expressed as the amount of PS (mg) encapsulated per 100 mg of nanoassembly; [b]ratio between actual and theoretical loading x 100.

ZnPc/SC16OH displayed a hydrodynamic diameter around 200 nm with an unimodal size distribution. Size and absence of macroscopic aggregation were confirmed by TEM microscopy (Figure 1). A negative value of zeta potential suggested a great stability of colloidal dispersions in water due to organization of the oligo-ethylene moieties on the surface, in line with our previous findings.[34] Concerning entrapment, ZnPc was incorporated in the nanoassembly with an efficiency as high as 76%. ZnPc/SC16OH could be dispersed in water up to 10 % w/v corresponding to a ZnPc entrapped amount around 152 μg/mL which is in line with that found in Cremophor EL, a highly toxic intravenous vehicle for administering lipophilic drugs.[35]
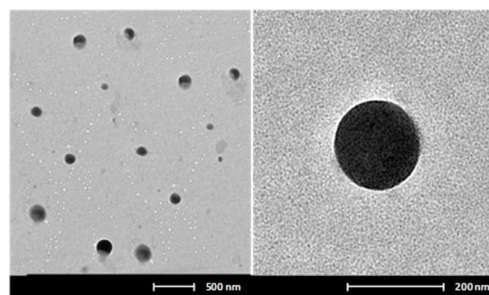

Figure 1. TEM images of ZnPc/SC16OH nanoassembly.

Releases studies on ZnPc/SC16OH shown in Figure 2 demonstrated that ZnPc was partially released with a sustained pattern only in the presence of a 10 % v/v of polysorbate 80 in the external medium acting as PS solubilizer. As reported in an our previous study,[34] the crystalline nature and the progressive dissolution of SC16OH nanoassembly contributed to modulated release of entrapped molecules, thus suggesting a release mechanism based on diffusion and progressive dissolution of nanoparticles.
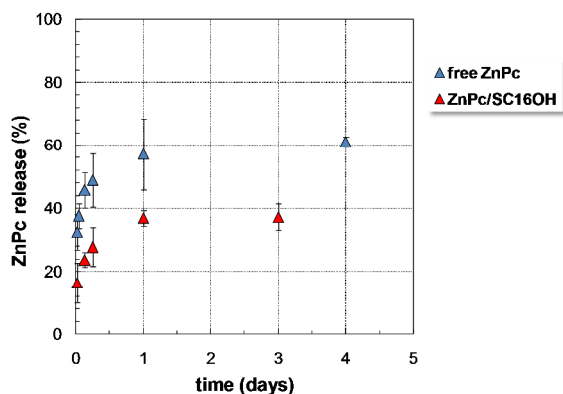

Figure 2. Release profile of ZnPc from ZnPc/SC16OH dispersed in a PBS at pH 7.4. External medium was PBS at pH 7.4 enriched with 10 % v/v of polysorbate 80 to ensure sink conditions. Release profile of ZnPc at the same concentration of that present inside ZnPc-nanoassembly is reported for comparison (insets). Data are reported as mean of three independent experiments ± SD.

Morphological and spectroscopic studies on ZnPc/SC16OH nanoassembly

Morphology of ZnPc/SC16OH nanoassembly was investigated by SNOL technique (Figure 3). The experimental setup allowed collection of both the topography and the optical response of the sample at the same time. From topography images (1.75 x 1.75 μm) (Figure 3 left), a structure consisting in a number of substructures with dimensions ranging between 100 and 300 nm was identified, confirming size measurements obtained by PCS and TEM. The optical images (Figure 3 right) showed a number of intense spots superimposed to a large diffused luminescence. Moreover, only part of the substructures gave luminescence which was mainly visible on layers of the nanoassemblies, possibly deriving from PS embedded in those regions of the amphiphile.
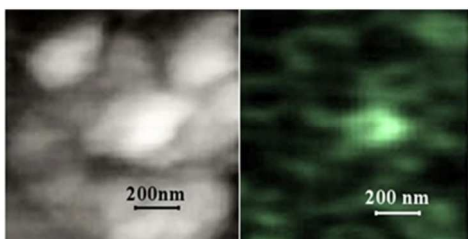

Figure 3. Topography images (left) and Luminescence images (right) from SNOL (λ_{ex}= 532 nm) on a sample drop-casted onto Si (100) surface from an aqueous dispersion of ZnPc/SC16OH (0.5 mg/mL).

In parallel, steady-state fluorescence emission spectra (Figure 4A) on samples prepared by dispersing an appropriate amount of powder in water were carried out. Figure 4A shows the emission spectrum of ZnPc/SC16OH in aqueous solution mainly characterized by bands centered at $\cong$ 680, 710 nm which are typical of metal-phthalocyanines. The excitation spectra of ZnPc/SC16OH (Figure 4B) showed the peculiar Q band centered at 672 nm which is typical of monomeric ZnPc. Both spectroscopic evidences indicate the good dispersion of the hydrophobic PS in aqueous solution, due to the entrapment in SC16OH.
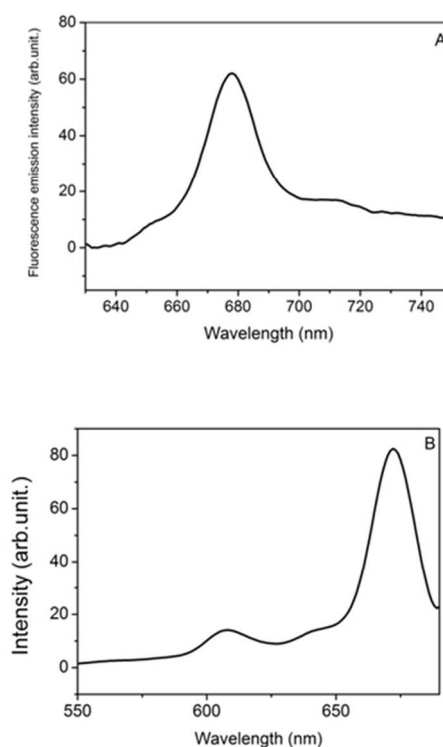

Figure 4: Steady-state fluorescence emission (A) and excitation spectra (B) of an aqueous dispersion of ZnPc/SC16OH: in A and B ZnPc concentration was fixed at 0.25 μg/mL, λ_{ex}= 600 nm (A), λ_{em}= 700 nm (B).

It is widely recognized that phthalocyanines, as well as other lipophilic PS, suffer strong aggregation in different media, thus forming oligomers with low triplet ~~oxygen~~ quantum yield and photodynamic efficacy. In order to clarify the interaction of ZnPc with SC16OH inside nanoassembly, time-resolved fluorescence and anisotropy were measured. From fluorescence time decay (Figure S1A), it results that free ZnPc in DMSO has a lifetime of 3 ±0.4 ns, and this value remains unaffected when ZnPc is entrapped in the nanoassembly. Fluorescence lifetime indicates that ZnPc is plausibly entrapped in monomeric form,[36] as already evidenced in the excitation spectra (Figure 4B). The longer rotational correlation time >20 ns, Supplementary

material S1B) in ZnPc/SC16OH as compared to ZnPc in DMSO ($\tau_R \cong 0.6$ ns and a limiting anisotropy of 0.05) was due to the fact that the dye is rotating together with larger particles. The similar fluorescence lifetime of ZnPc (3 ± 0.4 ns) in organic solvents (both in dichloromethane/THF mixture used in nanoassembly preparation and in DMSO)[36] and in the nanoassembly, suggests that clusters of residual organic solvent could assist the drug interaction in the mesoporous structure of nanoassembly.[37]

Investigation of ZnPc complexation in SC16OH

In order to elucidate the complexation phenomena between ZnPc and SC16OH, fluorescence emission of nanoassembly in organic solvents was evaluated (see Figure S2). The steady-state fluorescence emission spectrum of ZnPc/SC16OH dissolved in CHCl$_3$ appears similar to that of aqueous dispersion of ZnPc/SC16OH (after scattering correction). Altogether these results suggest that ZnPc in CHCl$_3$ preserves tendency to interact with CDs matrix, as suggested by anisotropy value of ZnPc at λ_{em} maximum ($\rho \cong 0.07$). On the other hand, ZnPc/SC16OH complex could be mostly dissociated in DMSO ($\rho \cong 0.02$).

In an attempt to distinguish interaction sites and to get insights on supramolecular structure, ^{1}H-NMR studies on ZnPc/SC16OH nanoassembly in CDCl$_3$ were performed.[38] First of all, ^{1}H-NMR spectrum of ZnPc/SC16OH nanoassembly in CDCl$_3$ (Figure 5A) was compared with that of free ZnPc in d$_6$-DMSO (Figure 5C), as free ZnPc is not soluble in CDCl$_3$. The ^{1}H-NMR spectrum of free ZnPc in d$_6$-DMSO (Figure 5C) showed signals at 8.27 and 9.44 ppm, assigned to protons in β- and α- positions, respectively.

From ^{1}H-NMR of ZnPc/SC16OH nanoassembly in CDCl$_3$ (Figure 5A) no detectable shifts of the signals of CD (which are fairly broad because of presumable formation of aggregates in CDCl$_3$) were registered. On the other hand, more than two signals were found for both protons of ZnPc in ZnPc/SC16OH (Figure 5B). In particular, the α- protons show resonances at 9.50 and 9.78 ppm, and those in β- position at 8.10 and 8.20 ppm, respectively. These findings evidenced how PS can be allocated in portions of SC16OH with different polarity. Indeed, we believe that both the oligo-ethyleneglycol and the thioalkyl moieties of SC16OH may host ZnPc.
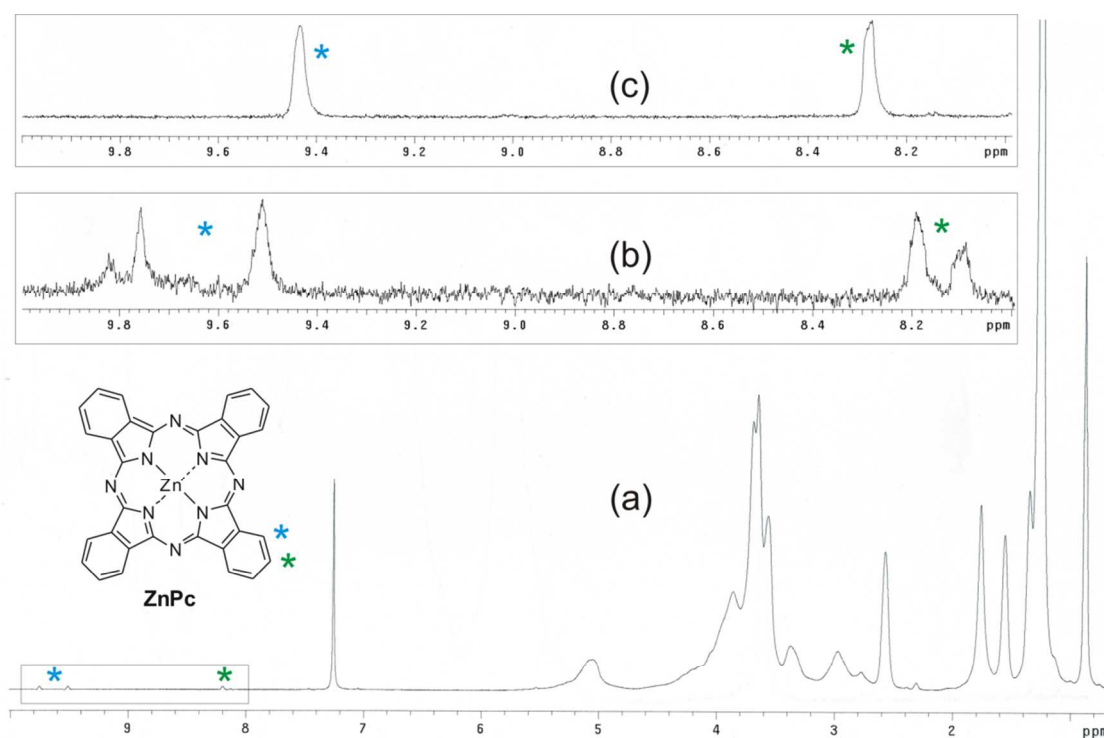

Figure 5: ^{1}H -NMR spectra of ZnPc/ SC16OH nanoassembly in CDCl$_3$ (T= 25°C) (A). The insets report a magnification of ZnPc signals of ZnPc/SC16OH in CDCl3 (B) and free ZnPc in d$_6$-DMSO (C).

Singlet oxygen generation and biological investigation of ZnPc/SC16OH nanoassembly

It is well recognized that biological activity of ZnPc, as well as of PS employed in PDT, is strictly related to photoinduced production of cytotoxic singlet oxygen, which is the main responsible of cellular damage. In general, the presence of a monomeric form of PS inside nanoassembly hampers aggregation in aqueous media as well as preserves its fluorescence and phosphorescence properties. On this premise, a semiquantitative evaluation of singlet oxygen production was carried out in order to confirm that ZnPc embedded in nanoassembly could release singlet oxygen upon appropriate irradiation. In Figure 6, the ADPA bleaching at 400 nm due to the production of singlet oxygen under irradiation from ZnPc-containing nanoassembly is shown.
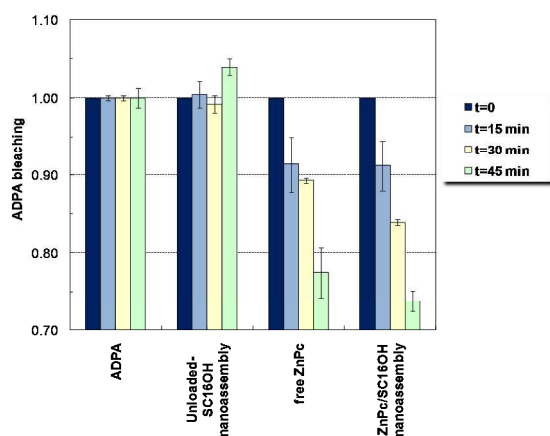

Figure 6. ADPA bleaching at 400 nm due to singlet oxygen generated from ZnPc-loaded nanoassembly dispersed in water (1 mg/mL) upon photoirradiation at 610 nm. ZnPc concentration was fixed at 2 μg/mL.ZnPc and unloaded nanoassembly are shown as control. Data are reported as ratio between sample OD after irradiation (OD_{irr}) and sample OD before irradiation (OD) and are the mean of three independent experiments ± SD.

In particular, a comparable time-dependent production of singlet oxygen was found for free ZnPc and ZnPc/SC16OH. These data are in line with previous results obtained with similar nanoassembly made of amphiphilic block copolymers recently developed.[30] Therefore, it is possible to conclude that the irradiation can photochemically activate ZnPc, also if entrapped in a nanocontainer, following production of singlet oxygen which can diffuse through the amphiphilic matrix and react with the external environment.

Having ascertained the photodynamic potential of ZnPc-loaded nanoassembly to produce cytotoxic singlet oxygen, its biological behaviour, in terms of cellular uptake and cytotoxicity, was investigated in HeLa cancer cells.

Due to the low actual loading of ZnPc into nanoassembly with a consequently low sensibility in detecting ZnPc emission, the uptake of nanoassembly in HeLa cells was traced after replacing ZnPc with Nile-Red (Nr/SC16OH nanoassembly).

Overall properties of Nr/SC16OH nanoassembly were very similar to those of ZnPc/SC16OH (Supplementary material S3). HeLa cells were treated with Nr/SC16OH and incubated for 1 hour at 37°C and 4°C, separately (Figure 7). Cells incubated at 37°C (Figure 7A) showed the red emitting nanoassembly inside macro-nanoassembly disseminated into the cytoplasm. On the other hand, weak emission signal in cells incubated at 4°C (Figure 7B) indicated that the treatment at lower temperature impairs the internalization of fluorescent nanoassembly. Thus, nanoassembly can be internalized in HeLa cells and the uptake was mediated by endocytosis, which is strongly inhibited at low temperatures.[39]
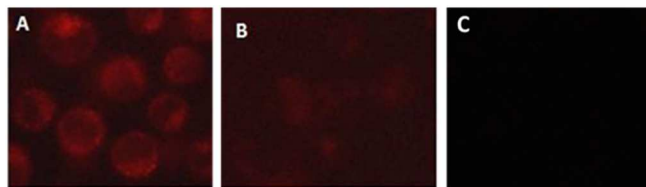

Figure 7. Fluorescence microscopy analysis of HeLa cells treated with Nr-nanoassembly at 37°C and 4°C (A and B respectively).and mock treated at 37 °C (C). Cells were incubated with Nr-nanoassembly, and analyzed 1 h post-exposure. Detection of Nr-nanoassembly in cells: Images were obtained by taking single exposures through bandpass optical filter appropriate for Nile Red (red).

To evaluate the biological effect of ZnPc/SC16OH, the percentage of viable HeLa cells after different times from treatment was measured (Figure 8). A slight reduction in terms of viability was detected in samples incubated with unloaded nanoassembly (from ~100 % to ~87% of cell viability) at all tested experimental times.
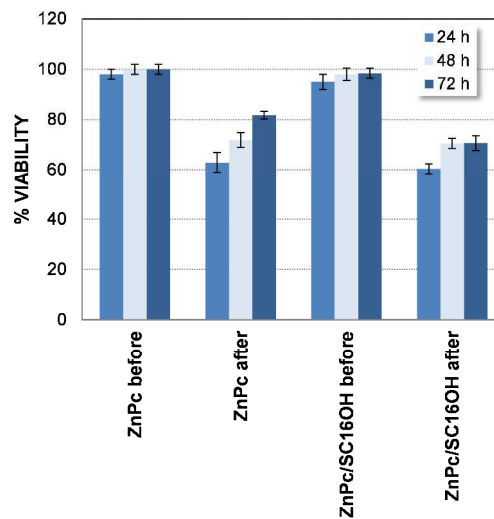

Figure 8. Effects of ZnPc and ZnPc/SC16OH on HeLa cells viability at 24, 48 and 72 h. Free ZnPc was used at the same concentrations present in the loaded nanoassembly (ZnPc concentration was set at 0.012 μg/mL in all the samples). Cell viability was quantified before (dark) and after (light) irradiation by using MTT assay.

ARTICLE

Variation of cell viability before and after irradiation was found after 24, 48 and 72 h upon treatment with free ZnPc and ZnPc/SC16OH was as effective as ZnPc in DMSO in inducing cell death thus suggesting that ZnPc inclusion in the cyclodextrin matrix did not affect significantly its biological behaviour. Nevertheless, maximum photodynamic activity was found after 24 h, in line with ZnPc mode of action,[35] which, at this time and upon irradiation, showed significant amount of ROS and activation of the molecular mechanisms of cell death.[35,40]

Several groups have investigated the photodynamic efficacy of free[35] and modified ZnPc,[41] ZnPc-loaded systems,[42] and ZnPc conjugates,[43] by elucidating their in *vitro* mechanism and in *vivo* biodistribution.[43] Interestingly, even if preliminar, our results show high PDT potential of nanoassembly based on ZnPc/SC16OH also at low low concentrations of entrapped ZnPc, similarly to not-nanoassembled cationic derivatives of ZnPc.[41]

However further investigations are necessary to gain more knowledge about the endocytic mechanisms and intracellular pathways utilized by nanoassembly based on these aCD, as well as a full understanding of how their properties can influence distribution in different cellular compartments where photodamage and cell death are generated.

Conclusions

In summary, this study has demonstrated that heptakis (2-Oligo(ethyleneoxide)-6-hexadecylthio-)-β-CD (SC16OH) and zinc(II)-phthalocyanine (ZnPc) form a suitable photosensitizing nanoassembly which delivers an highly lipophilic PS to cancer cells. Due to its amphiphilic features, in fact, SC16OH evidenced a propensity to assemble in biodegradable vesicles, allowing a strong interaction with ZnPc which is embedded in active monomeric form both in the hydrophobic and hydrophilic moieties of SC16OH. Under irradiation, the nanoassembly showed photodynamic effects on HeLa cancer cells comparable to that of free drug in DMSO thus pointing to its potential use in an in vivo setting.

Acknowledgements

Notes and references

ᵃ Department of Pharmacy, University of Napoli Federico II, Via Domenico Montesano 49, 80131 Napoli, Italy

ᵇ CNR-ISMN Institute of Nanostructured Materials c/o Dept. of Chemical Sciences of the University of Messina, V.le F. Stagno d'Alcontres 31, 98166 Messina, Italy

ᶜ Department of Biological and Environmental Sciences, University of Messina, Viale F. Stagno D'Alcontres 31,98166, Messina, Italy

ᵈ CNR-IPCF Institute for Chemical and Physical Processes ~~stituto~~, V.le F. Stagno d'Alcontres 37, Faro Superiore, 98166 Messina, Italy

ᵉ Department of Matter Physics and Electronic Engineering, University of Messina, V.le F. Stagno d'Alcontres 31 – 98166 Messina, Italy

Prof. Fabiana Quaglia: Tel/Fax: +39 81 678707; E-mail: quaglia@unina.it
Dr. Antonino Mazzaglia:Tel/Fax: +39 90 3974108; E-mail: antonino.mazzaglia@ismn.cnr.it

The authors declare no competing financial.

Supporting Information. Time-resolved fluorescence measurements (Figure S1); Depolarized fluorescence spectra (Figure S2).; Overall properties of Nr/SC16OH nanoassembly. ~~This material is available free of charge via the Internet at http://pubs.acs.org.~~"

References
1 P. Agostinis, K. Berg, K. A. Cengel, T. H. Foster, A. W. Girotti, S. O. Gollnick, S. M. Hahn, M. R. Hamblin, A. Juzeniene, D. Kessel, M. Korbelik, J. Moan, P. Mroz, D. Nowis, J. Piette, B. C. Wilson, J. Golab, CA *Cancer J. Clin*. 2011, **61**, 250.
2 M. Dewaele, T. Verfaillie, W. Martinet, P. Agostinis, in Photodynamic Therapy (Ed: C. J. Gomer), Humana Press 2010, 7.
3 A. Juarranz, P. Jaen, F. Sanz-Rodriguez, J. Cuevas, S. Gonzalez, *Clin. Transl. Oncol*. 2008, **10**, 148.
4 A. Wang, L. Long, C. Zhang, *J Incl Phenom Macrocycl Chem* 2011, **71**, 1.
5 N. Sekkat, H. van den Bergh, T. Nyokong, N. Lange, *Molecules*. 2012, **17**, 98.
6 T. Loftsson, M. E. Brewster, *Journal of Pharmacy and Pharmacology* 2010, **62**, 1607.
7 E. Memisoglu, A. Bochot, M. Sen, D. Charon, D. Duchene, A. A. Hincal, *J. Pharm. Sci*. 2002, **91**, 1214.
8 D. Duchene, D. Wouessidjewe, G. Ponchel, *J. Control Release* 1999, **62**, 263.
9 E. Bilensoy, A. A. Hincal, *Expert. Opin. Drug Deliv*. 2009, **6**, 1161.
10 M. Roux, B. Perly, F. Djedani-Pilard, *Eur Biophys J* 2007, **36**, 861.
11 L. Jiang, Y. Yan, J. Huang, *Advances in Colloid and Interface Science* 2011, **169**, 13.
12 F. Sallas, R. Darcy, *Eur. J. Org. Chem*. 2008, 957 and ref therein.
13 S. D. Baugh, Z. Yang, D. K. Leung, D. M. Wilson, R. Breslow, *J. Am. Chem. Soc*. 2001, **123**, 12488.
14 J. T. Lau, P. C. Lo, Y. M. Tsang, W. P. Fong, D. K. Ng, *Chem. Commun. (Camb.)* 2011, **47**, 9657.
15 A. R. Silva, A. R. Simioni, A. C. Tedesco, *J. Nanosci. Nanotechnol*. 2011, **11**, 4046.
16 J. Králová, Z. Kejík, T. Briza, P. Pouckova, A. Kral, P. Martasek, V. Kral, *J. Med. Chem*. 2009, **53**, 128.
17 H. Kolarova, J. Macecek, P. Nevrelova, M. Huf, M. Tomecka, R. Bajgar, J. Mosinger, M. Strnad, *Toxicol. In Vitro* 2005, **19**, 971.
18 D. Iohara, M. Hiratsuka, F. Hirayama, K. Takeshita, K. Motoyama, H. Arima, K. Uekama, *J. Pharm. Sci*. 2012, **101**, 3390.
19 A. B. Hegge, T. T. Nielsen, K. L. Larsen, E. Bruzell, H. H. Tonnesen, *J. Pharm. Sci*. 2012, **101**, 1524.
20 S. A. Sibani, P. A. McCarron, A. D. Woolfson, R. F. Donnelly, *Expert. Opin. Drug Deliv*. 2008, **5,** 1241.
21 D. K. Chatterjee, L. S. Fong, Y. Zhang, *Adv. Drug Deliv. Rev*. 2008, **60**, 1627.
22 J. Voskuhl, U. Kauscher, M. Gruener, H. Frisch, B. Wibbeling, C. A. Strassert, B. J. Ravoo, *Soft Matter* 2013, **9**, 2453.
23 S. Sortino, A. Mazzaglia, L. Monsù Scolaro, M. F. Marino, V. Valveri, M. T. Sciortino, *Biomaterials* 2006, **27**, 4256.
24 A. Mazzaglia, A. Valerio, N. Micali, V. Villari, F. Quaglia, M. A. Castriciano, L. M. Scolaro, M. Giuffre, G. Siracusano, M. T. Sciortino, *Chem. Commun. (Camb*.) 2011, **47**, 9140.
25 A. Mazzaglia, N. Angelini, D. Lombardo, N. Micali, S. Patan+®, V. Villari, L. M. Scolaro, *J. Phys. Chem. B* 2005, **109**, 7258.

26 N. Kandoth, E. Vittorino, M. T. Sciortino, T. Parisi, I. Colao, A. Mazzaglia, S. Sortino, *Chem. Eur. J.* 2012, **18**, 1684.

27 A. McMahon, M. J. O'Neil, E. Gomez, R. Donohue, D. Forde, R. Darcy, C. M. O'Driscoll, *J Pharm Pharmacol*. 2012, **64**, 1063.

28 J. H Schenkel, A Samanta, B. J. Ravoo, *Adv. Mater*. 2014, **26**, 1076.

29 A. Mazzaglia, R. Donohue, B. J. Ravoo, R. Darcy, Eur. J. Org. Chem. 2001, 1715.

30 C. Conte, F. Ungaro, G. Maglio, P. Tirino, G. Siracusano, M. T. Sciortino, N. Leone, G. Palma, A. Barbieri, C. Arra, A. Mazzaglia, F. Quaglia, *J. Control Release* 2013, **167**, 40.

31 J. R. Lackowicz, Principles of Fluorescence Spectroscopy, Kluwer Academic, Plenum Publisher, New York 1999.

32 N. Angelini, N. Micali, V. Villari, P. Mineo, D. Vitalini, E. Scamporrino, *Phys. Rev. E* 2005, *71*, 021915.

33 W. Tang, H. Xu, R. Kopelman, M. A. Philbert, *Photochem. Photobiol*. 2005, **81**, 242.

34 F. Quaglia, L. Ostacolo, A. Mazzaglia, V. Villari, D. Zaccaria, M. T. Sciortino, *Biomaterials* 2009, **30**, 374.

35 J. Shao, Y. Dai, W. Zhao, J. Xie, J. Xue, J. Ye, L. Jia, *Cancer Letters* 2013, **330**, 49.

36 J. Savolainen, D. van der Linden, N. Dijkhuizen, J. L. Herek, *J. Photochem. Photobiol. A.: Chem.*2008, **196**, 99.

37 R. Stancanelli, M. Guardo, C. Cannavá, G. Guglielmo, P. Ficarra, V. Villari, N. Micali, A. Mazzaglia, *J. Pharm. Sci.* 2010, **99**, 3141.

38 G. Ivanova, M. Simeonova, E. J. Cabrita, M. Rangel, *J. Phys. Chem. B* 2010, **115**, 902.

39 T. Haylett, L. Thilo, *J Biol. Chem* 1991, **266**, 8322.

40 G. H. Rodal, S. K. Rodal, J. Moan, K. Berg, *J Photochem Photobiol B*. 1998, **45**, 150.

41 S. Banfi, E. Caruso, L. Buccafurni, R. Ravizza, M. Gariboldi, E. Monti, *J. Organomet. Chem*., 2007, **692**,1269.

42 M. da Volta Soares, M. Rangel Oliveira, E. Pereira dos Santos, L. de Brito Gitirana, G. Moreno Barbosa, C. Holandino Quaresma, E. Ricci-Júnior, *Int J Nanomedicine*, 2011, **6**, 227.

43 M. Camerin, M. Magaraggia, M. Soncin, G. Jori, M. Moreno, I. Chambrier, M. J. Cook, D. A. Russell, *Eur. J. Cancer*, 2010, **46**, 1910.
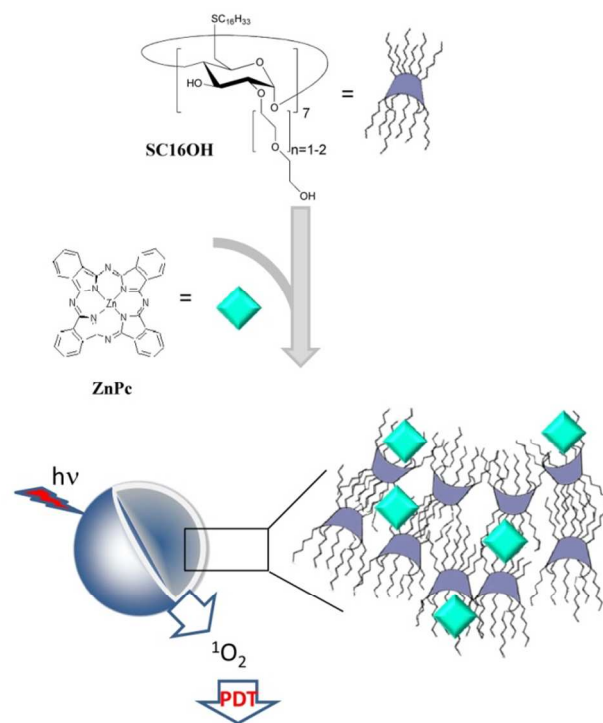
A photosensitising nanoassembly from non-ionic amphiphlic cyclodextrin and highy hydrophobic Zn-pthalocyanine with capability to sustain release of entrapped photosensitiser and showing photodynamic activity in cancer cell.